



**HAL**  
open science

## Selective dry etching of TiN nanostructures over SiO<sub>2</sub> nanotrenches using a Cl<sub>2</sub>/Ar/N<sub>2</sub> inductively coupled plasma

Bruno Lee Sang, Marie-Josée Gour, Maxime Darnon, Serge Ecoffey, Abdelatif Jaouad, Benattou Sadani, Dominique A Drouin, Abdelkader Souifi

► **To cite this version:**

Bruno Lee Sang, Marie-Josée Gour, Maxime Darnon, Serge Ecoffey, Abdelatif Jaouad, et al.. Selective dry etching of TiN nanostructures over SiO<sub>2</sub> nanotrenches using a Cl<sub>2</sub>/Ar/N<sub>2</sub> inductively coupled plasma. *Journal of Vacuum Science and Technology*, 2016, 34 (2), 10.1116/1.4936885 . hal-01701405

**HAL Id: hal-01701405**

**<https://hal.science/hal-01701405>**

Submitted on 3 May 2024

**HAL** is a multi-disciplinary open access archive for the deposit and dissemination of scientific research documents, whether they are published or not. The documents may come from teaching and research institutions in France or abroad, or from public or private research centers.

L'archive ouverte pluridisciplinaire **HAL**, est destinée au dépôt et à la diffusion de documents scientifiques de niveau recherche, publiés ou non, émanant des établissements d'enseignement et de recherche français ou étrangers, des laboratoires publics ou privés.

# Selective dry etching of TiN nanostructures over SiO<sub>2</sub> nanotrenches using a Cl<sub>2</sub>/Ar/N<sub>2</sub> inductively coupled plasma

Bruno Lee Sang, Marie-Josée Gour, Maxime Darnon, Serge Ecoffey, Abdelatif Jaouad, Benattou Sadani, Dominique Drouin, and Abdelkader Souifi

Citation: *Journal of Vacuum Science & Technology B, Nanotechnology and Microelectronics: Materials, Processing, Measurement, and Phenomena* **34**, 02M102 (2016); doi: 10.1116/1.4936885

View online: <http://dx.doi.org/10.1116/1.4936885>

View Table of Contents: <http://avs.scitation.org/toc/jvb/34/2>

Published by the [American Vacuum Society](#)

---

## Articles you may be interested in

[Dry etching characteristics of TiN film using Ar/CHF<sub>3</sub>, Ar/Cl<sub>2</sub>, and Ar/BCl<sub>3</sub> gas chemistries in an inductively coupled plasma](#)

*Journal of Vacuum Science & Technology B: Microelectronics and Nanometer Structures Processing, Measurement, and Phenomena* **21**, 2163 (2016); 10.1116/1.1612517

[Characterization of titanium nitride etch rate and selectivity to silicon dioxide in a Cl<sub>2</sub> helicon-wave plasma](#)

*Journal of Vacuum Science & Technology A: Vacuum, Surfaces, and Films* **19**, 455 (2001); 10.1116/1.1342866

[Dry-etching properties of TiN for metal/high-\*k\* gate stack using BCl<sub>3</sub>-based inductively coupled plasma](#)

*Journal of Vacuum Science & Technology A: Vacuum, Surfaces, and Films* **27**, 1320 (2009); 10.1116/1.3244567

[Performance of different etch chemistries on titanium nitride antireflective coating layers and related selectivity and microloading improvements for submicron geometries obtained with a high-density metal etcher](#)

*Journal of Vacuum Science & Technology A: Vacuum, Surfaces, and Films* **15**, 702 (1998); 10.1116/1.580805

[Dry etching of titanium nitride thin films in CF<sub>4</sub>-O<sub>2</sub> plasmas](#)

*Journal of Vacuum Science & Technology A: Vacuum, Surfaces, and Films* **13**, 335 (1998); 10.1116/1.579419

[Etching characteristics of TiN used as hard mask in dielectric etch process](#)

*Journal of Vacuum Science & Technology B: Microelectronics and Nanometer Structures Processing, Measurement, and Phenomena* **24**, 2262 (2016); 10.1116/1.2338048

---



## Instruments for Advanced Science

Contact Hiden Analytical for further details:

**W** [www.HidenAnalytical.com](http://www.HidenAnalytical.com)

**E** [info@hiden.co.uk](mailto:info@hiden.co.uk)

**CLICK TO VIEW** our product catalogue



### Gas Analysis

- › dynamic measurement of reaction gas streams
- › catalysis and thermal analysis
- › molecular beam studies
- › dissolved species probes
- › fermentation, environmental and ecological studies



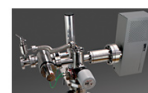
### Surface Science

- › UHV TPD
- › SIMS
- › end point detection in ion beam etch
- › elemental imaging - surface mapping



### Plasma Diagnostics

- › plasma source characterization
- › etch and deposition process reaction
- › kinetic studies
- › analysis of neutral and radical species



### Vacuum Analysis

- › partial pressure measurement and control of process gases
- › reactive sputter process control
- › vacuum diagnostics
- › vacuum coating process monitoring

# Selective dry etching of TiN nanostructures over SiO<sub>2</sub> nanotrenches using a Cl<sub>2</sub>/Ar/N<sub>2</sub> inductively coupled plasma

Bruno Lee Sang,<sup>a)</sup> Marie-Josée Gour, Maxime Darnon, Serge Ecoffey, Abdelatif Jaouad, Benattou Sadani, and Dominique Drouin

*Institut Interdisciplinaire d'Innovation Technologique (3IT), Université de Sherbrooke 3000 Boul. Université, Sherbrooke, Québec J1K 0A5, Canada and Laboratoire Nanotechnologies Nanosystèmes (LN2) - CNRS UMI-3463, Université de Sherbrooke, Québec J1K 0A5, Canada*

Abdelkader Souifi

*Institut des Nanotechnologies de Lyon - UMR CNRS 5270, 7 av. Jean Capelle, 69621 Villeurbanne Cedex, France*

(Received 25 August 2015; accepted 17 November 2015; published 2 December 2015)

An inductively coupled plasma etch process for the fabrication of TiN nanostructures over nanotopography is presented. Using a Cl<sub>2</sub>/Ar/N<sub>2</sub> plasma, a selectivity of 50 is achieved over SiO<sub>2</sub>. The effect of N<sub>2</sub> flow rate on the etch rates and the nonvolatile residues on TiN sidewalls is investigated. As N<sub>2</sub> flow rate is increased up to 50 sccm, a change in the deposition of the nonvolatile residues on TiN sidewalls is observed. The current density–voltage characterizations of TiN devices fabricated with TiN nanostructure sidewalls are presented. The measured current densities of two different samples etched with low and high N<sub>2</sub> flow rate, respectively, demonstrated the presence after cleaning of an insulating layer deposited on the sidewalls for low N<sub>2</sub> flow rate only. © 2015 American Vacuum Society. [<http://dx.doi.org/10.1116/1.4936885>]

## I. INTRODUCTION

Titanium nitride (TiN) is a multipurpose material because it presents a high compatibility with high-k dielectrics, a low electrical resistivity, and a good chemical stability. Among other applications, it is used as metal gate electrode, diffusion barrier, adhesive layer, or hard mask<sup>1–4</sup> in very large scale integration. TiN etching raises many challenges such as having high selectivity over mask and under layers, controlling the etch profiles and the generation of nonvolatile residues. In single electron transistor (SET) fabrication with a fabrication process similar to the nanodamascene process,<sup>5</sup> TiN nanostructures have to be etched over nanotopography with passivation-free sidewalls after cleaning in order to obtain high-quality tunnel junctions. Dry etching characteristics of TiN thin films with halogen gases (CHF<sub>3</sub>, BCl<sub>3</sub>, and Cl<sub>2</sub>) and additional gases (Ar, N<sub>2</sub>, O<sub>2</sub>, and He) have been widely investigated.<sup>6–11</sup> The Cl-based plasmas are more commonly used than F-based plasmas due to the lower boiling point of the volatile byproducts, 136.5 °C for TiCl<sub>4</sub> and 284 °C for TiF<sub>4</sub>.<sup>10</sup> They also provide a better selectivity with SiO<sub>2</sub> than F-based plasmas.<sup>12</sup> In addition, TiF<sub>x</sub> species formed during F-based etching processes may form residues when they react with water in clean room atmosphere.<sup>13</sup> It is also reported that BCl<sub>3</sub> plasmas can form nonvolatile BN<sub>x</sub> compounds on surface.<sup>14</sup> Only few processes have been reported on the selective etching of TiN nanostructures, and HBr gas is generally used due to its high selectivity over common gate oxides.<sup>15,16</sup>

In this work, a dry etching process is proposed for the fabrication of TiN nanostructures with high selectivity over silicon oxide nanopatterns using a Cl<sub>2</sub>/Ar/N<sub>2</sub>-based inductively coupled plasma (ICP). The effect of N<sub>2</sub> flow rate on

the etch rates and the nonvolatile residues on sidewalls is investigated. Electrical results of TiN devices etched with low and high nitrogen flow rates are presented in order to exhibit the presence of an insulating layer on the nanostructure sidewalls.

## II. EXPERIMENTAL SETUP AND METHODOLOGY

A 150 nm-thick layer of SiO<sub>2</sub> is thermally grown on Si substrate and 1 × 1 cm samples are diced for process development. A 25 nm-thick TiN layer is deposited on the samples by sputtering. To obtain microstructured samples, a positive photoresist S1805 from Dow Chemical is spun at 5000 rpm and baked at 115 °C for 1 min. The resist is exposed with a photomask for 4.5 s and developed in MF-319 from Dow Chemical for 1 min. The lamp used for exposure produces light from 220 to 436 nm. An oxygen plasma descum of 30 s is done after development to remove residues on exposed surfaces. To obtain nanostructured samples, an electron beam resist ZEP520A from Zeon Chemicals, diluted with a ratio of 1.7:1 with anisole, is spun at 5000 rpm and baked at 180 °C for 5 min to obtain a 200 nm-thick layer. Grating structures are exposed at 50 μC/cm<sup>2</sup> area dose using a 20 keV energy beam, then developed in O-xylene for 75 s, and rinsed in methyl isobutyl ketone solution. Unpatterned 200 nm-thick ZEP samples and 150 nm-thick TiN samples patterned with S1805 have also been prepared to carry out etch rate measurements.

Samples are placed on a 200 mm diameter Si wafer and introduced in a STS Multiplex III–V ICP system. Two separate 13.56 MHz RF sources are connected to the coil and the chuck to generate the plasma and control the ion energy, respectively. During processing, the wafer placed on the chuck can be cooled or heated allowing the variation of the wafer temperature. The experiments are carried out with

<sup>a)</sup>Electronic mail: [bruno.lee.sang@usherbrooke.ca](mailto:bruno.lee.sang@usherbrooke.ca)

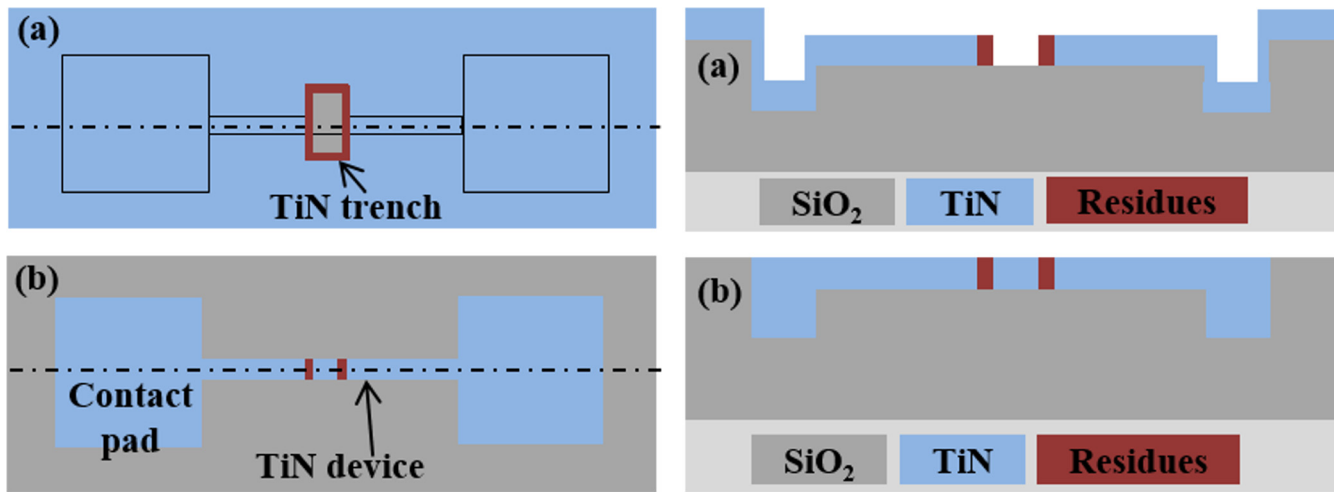


Fig. 1. (Color online) Illustrations of top view on the left and cross-section on the right: (a) after TiN nanostructure etching over a SiO<sub>2</sub> nanotrench and (b) after filling and sample planarization.

these starting conditions: 225 W coil power, 16 W platen power, 5 mTorr pressure, 5 sccm Cl<sub>2</sub> flow rate, 5 sccm Ar flow rate, 5 sccm N<sub>2</sub> flow rate, and -20 °C platen temperature. The etch time is fixed at 2 min to determine the etch rates. N<sub>2</sub> flow rate is varied from 5 to 50 sccm during the experiments while the other parameters are fixed to study its influence on the etch rates and the nonvolatile residues on sidewalls. In order to investigate the nonvolatile residues on sidewalls after etching, TiN patterned samples are cleaned subsequently with Remover 1165 from Dow Chemicals, acetone, isopropanol, and deionized (DI) water, and finally etched in a 30% H<sub>2</sub>O<sub>2</sub> solution at 70 °C for 5 min.<sup>17</sup> TiN is etched by H<sub>2</sub>O<sub>2</sub> while most potential nonvolatile residues (TiO<sub>x</sub>, CCl<sub>x</sub>, and SiO<sub>x</sub>) are not. Thus, the presence of any residues after wet etching would illustrate the presence of nonvolatile residues on TiN sidewalls.

To electrically characterize the sidewalls of TiN after etching, TiN test structures similar to single electron transistors with a source, a drain, and an island are fabricated. The presence of an insulating layer on the TiN sidewalls would result in metal-insulator-metal (MIM) junctions, with nonlinear J-V characteristics. If the sidewalls are clean, the test structure should behave as a nanowire with a linear J-V characteristic. SiO<sub>2</sub> samples are patterned and etched with the process

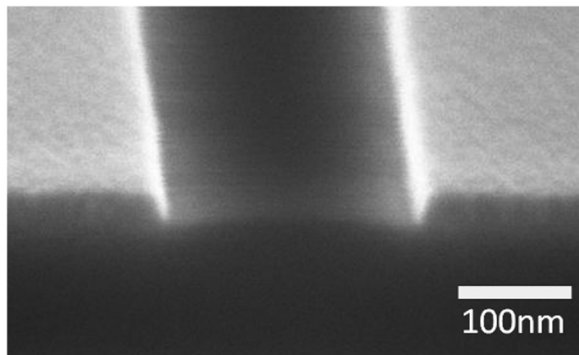


Fig. 2. Twenty-five nanometers deep TiN nanotrench etched on a SiO<sub>2</sub> substrate.

developed by Guilmain *et al.*<sup>18</sup> to create contact electrodes and 20 nm-deep nanotrenches into the SiO<sub>2</sub> layer. After depositing a 25 nm-thick TiN blanket film, a nanotrench is patterned by e-beam lithography and etched into the TiN to form a nanotrench perpendicular to the SiO<sub>2</sub> nanotrenches, as shown in Fig. 1(a). After TiN etching, a thick TiN blanket film is deposited to fill the trenches, and the test structures are planarized by chemical-mechanical planarization, as shown in Fig. 1(b). Four point probe measurements have been used to determine the device resistance between the two contact pads.

ZEP etch rates are obtained by measuring with a spectroscopic ellipsometer the thicknesses of unpatterned ZEP samples before and after etching. The model used for the ZEP layer is a Cauchy model. The depth of TiN microstructures is measured by profilometry after etching and resist cleaning steps in order to obtain TiN etch rates. Scanning electron microscope (SEM) is used to observe the cross-section of TiN structures.

### III. RESULTS AND DISCUSSION

#### A. Etching of TiN nanostructures on nanotopography

For the fabrication of the TiN nanostructures, a Cl<sub>2</sub>/Ar/N<sub>2</sub> gas mixture is used to etch TiN thin film selectively over SiO<sub>2</sub>. Figure 2 shows a TiN nanotrench completely etched on a clean SiO<sub>2</sub> surface, with the etching conditions presented in Table I. With these conditions, the etch rates

TABLE I. Etching conditions.

Parameters	
Cl <sub>2</sub> (sccm)	5
Ar (sccm)	5
N <sub>2</sub> (sccm)	5
Coil power (W)	225
Platen power (W)	16
Pressure (mTorr)	5
Platen temperature (°C)	-20

for TiN and SiO<sub>2</sub> are 66 and 1.3 nm/min, respectively, corresponding to a selectivity of 50. Cl<sub>2</sub> flow rate is kept at a minimum of 5 sccm because increasing Cl<sub>2</sub> flow rate would increase the TiN etch rate,<sup>19</sup> which is not wanted here. Argon is added in order to dilute Cl<sub>2</sub> gas and reduce the ratio between the reactive species (Cl) and ions.<sup>20</sup>

TiN nanostructures etching is also done over SiO<sub>2</sub> patterned samples, as shown in Fig. 3(a). A 60 nm wide TiN trench, perpendicular to a 30 nm-wide and 20 nm-deep SiO<sub>2</sub> trench, is entirely etched. Even though TiN etch rate is 66 nm/min, 2.5 min are needed to completely etch the 25 nm-thick TiN on the SiO<sub>2</sub> surface inside the nanotrench. ZEP resist is 200 nm-thick before etching, and reactive ion etching lag can be the reason for this longer etch time.<sup>21</sup> Figure 3(b) shows an AFM image of a sample after trench filling and planarization. TiN patterns are higher than SiO<sub>2</sub> surface due to the difference in the material removal rates. The current density–voltage measurements of the TiN device are used to verify the presence of an insulating layer deposited on the TiN sidewalls. The results are presented in Sec. III C.

### B. Effect of N<sub>2</sub> gas flow on etch rates and nonvolatile residues

To study the impact of N<sub>2</sub> gas on TiN etching, TiN microstructures are etched using different flow rates of N<sub>2</sub> in the Cl<sub>2</sub>/Ar mixture with other etching parameters fixed. The

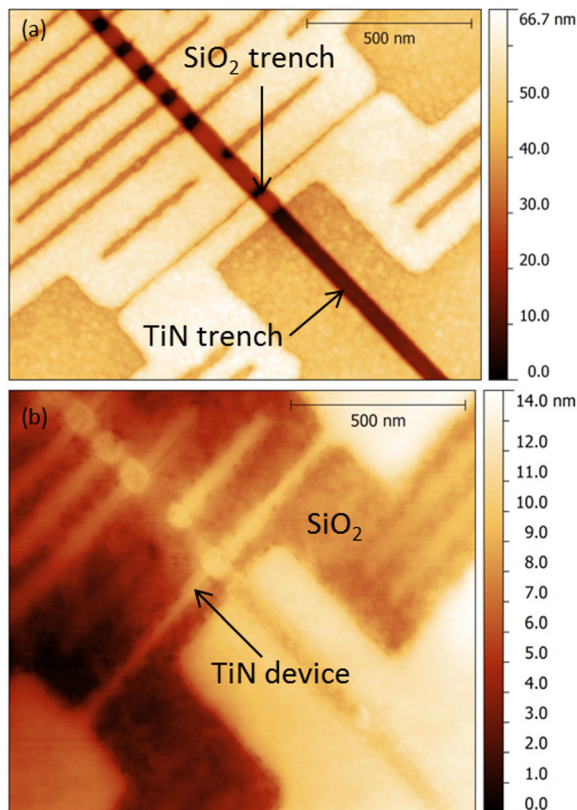


Fig. 3. (Color online) (a) AFM image of a TiN nanotrench etched over SiO<sub>2</sub> nanotrenches. (b) AFM image of the same sample after filling and planarization.

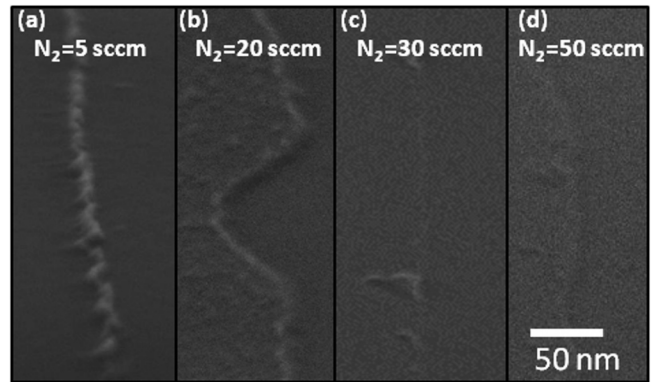


Fig. 4. Tilted SEM images after H<sub>2</sub>O<sub>2</sub> wet etch of dry etched TiN structures as a function of the additive N<sub>2</sub> flow rate: (a) 5 sccm, (b), 20 sccm, (c) 30 sccm, and (d) 50 sccm.

samples are etched in a 30% H<sub>2</sub>O<sub>2</sub> solution to reveal materials that are not TiN. Figure 4 shows the sidewall of microstructures etched with different N<sub>2</sub> flow rates after H<sub>2</sub>O<sub>2</sub> etching. One can observe that when TiN is etched with 5 sccm of N<sub>2</sub> in Fig. 4(a), there are some residues left. However, as N<sub>2</sub> flow rate increases from 5 to 30 sccm, these residues become less apparent. Finally, at 50 sccm, a clean surface with a SiO<sub>2</sub> step due to the over etch is observed. Moreover, Fig. 5 shows TiN, ZEP, and SiO<sub>2</sub> etch rates, and self-bias voltage in inset as a function of N<sub>2</sub> flow rate. From 5 to 50 sccm, TiN and ZEP etch rates decrease. SiO<sub>2</sub> etch rate slowly increases from 0 to 20 sccm and then stabilizes for larger N<sub>2</sub> flow rates. Similarly, the platen self-bias increases as the N<sub>2</sub> flow rate increases to 20 sccm, and then it stabilizes at 84 V for higher N<sub>2</sub> flow rates.

For TiN etching in Cl<sub>2</sub> plasmas, the etch mechanism reported is ion enhanced chemical etching.<sup>10,22</sup> Cl radicals react with Ti and N to produce TiCl<sub>x</sub> and NCl<sub>x</sub> products, which can be volatile products with the assistance of ion bombardment. It has been reported that N<sub>2</sub> addition in chlorine plasmas can either increase or decrease TiN etch rate depending on the plasma conditions;<sup>6,8,10</sup> however, no clear

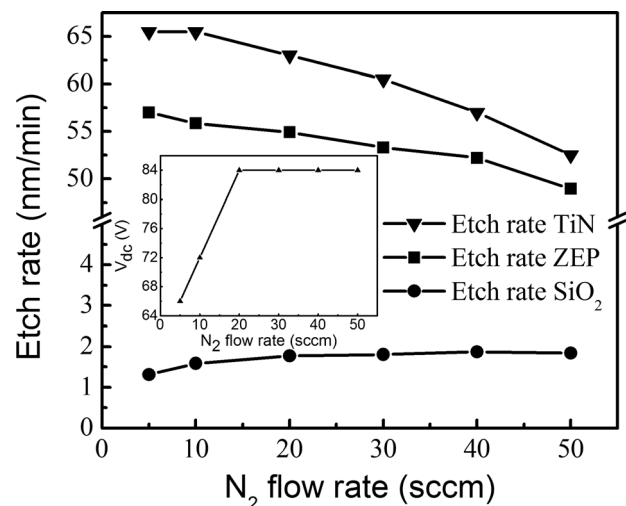


Fig. 5. TiN, ZEP, and SiO<sub>2</sub> etch rates as a function of N<sub>2</sub> flow rate. Inset: Self-bias voltage as a function of N<sub>2</sub> flow rate.

explanation has been given regarding the role of  $N_2$ . In our experiments, TiN etch rate decreases as  $N_2$  flow rate increases. Two possible mechanisms are proposed to explain this result. The first one is based on ion bombardment. From 5 to 20 sccm, the self-bias voltage increases while the platen power is fixed. It means that ion energy increases but it is compensated by the decrease in the ion flux. Second, for a large introduction of  $N_2$  gas, an effect of plasma dilution is dominant, and therefore, it reduces the density of chlorine species and TiN etch rate.

The reduction in nonvolatile residues after wet etching, as nitrogen flow rate increases, can be explained by two different hypotheses. (1) Adding nitrogen in the plasma prevents the formation of nonvolatile residues at TiN sidewalls. In this case, lateral etching of TiN would be expected.<sup>15</sup> Since we did not observe trench width increase during the process, we can rule out this hypothesis. (2) Adding nitrogen in the plasma changes the nature of the nonvolatile residues that desorb after the etch process, or become soluble either in solvents used for cleaning or in  $H_2O_2$ . There are several possible known nonvolatile residues, which can be deposited, such as  $TiO_xN_y$ ,  $SiO_x$ , or  $CO_xCl_y$ .<sup>15,23,24</sup> As mentioned earlier, these components are not soluble in  $H_2O_2$ . As  $N_2$  gas flow increases, the formation of  $TiO_xN_y$  could be reduced due to the reaction of nitrogen with oxygen to form nitric oxide.  $SiO_x$  species come from silicon oxide etching and could become  $SiO_xN_y$  by reacting with nitrogen. But  $SiO_xN_y$  is not etched by solvents; therefore, nonvolatile residues on sidewalls are probably not composed of  $SiO_xN_y$ . The formation of  $CO_xCl_y$  is due to the resist etching.<sup>23</sup> In Fig. 5, ZEP etch rate is reduced when  $N_2$  flow rate is increased. It means that less etch byproducts are formed because the etch time is fixed for any  $N_2$  flow rates. Moreover, when the nitrogen flow rate increases, the formation of  $CCl_x$  layer may be more dominant because of the oxygen reduction with nitrogen. Then, when  $CCl_x$  is in contact with the air, volatile products as CO and  $CO_2$  may form, leaving the sidewall without nonvolatile residues. Based on this discussion, one could say that nonvolatile residues formed at the TiN sidewalls become soluble in solvents or volatile upon exposure to the atmosphere when  $N_2$  is added in the plasma. However, it cannot be confirmed without chemical composition analyses of the nonvolatile residues.

### C. Electrical characterizations of TiN devices

Two different TiN devices are fabricated as described in Sec. III A with different TiN etching conditions. The TiN nanotrench for the first device is etched with a  $N_2$  flow rate of 5 sccm while the second one is etched with 50 sccm. Etch time is maintained at 2.5 min for both experiments. Figure 6 shows the current density–voltage characteristics of the two devices. By measuring the width of the device with an AFM and by extracting the device depth with a resistivity to thickness model,<sup>25</sup> the current is normalized to obtain the current density. The device etched with 50 sccm of  $N_2$  presents a linear resistor-like curve and a very high current density ( $10^6 A/cm^2$ ) whereas the other device presents lower current

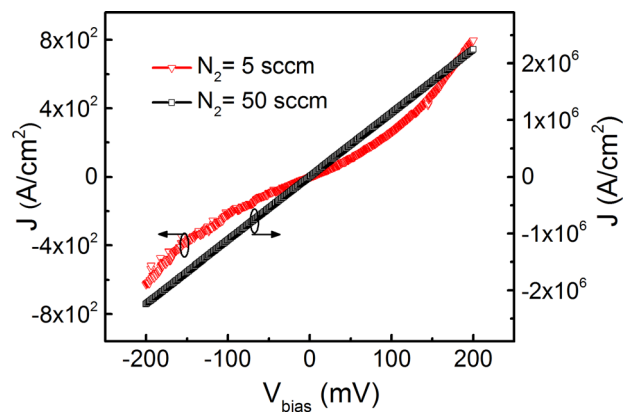


Fig. 6. (Color online) J-V curves of two devices. Squares and triangles represent two samples etched with  $N_2 = 50$  sccm and  $N_2 = 5$  sccm, respectively, in addition to the  $Cl_2/Ar$  mixture.

density ( $10^2 A/cm^2$ ) and a nonlinear J-V characteristic. During the TiN etching in the  $SiO_2$  nanotrench, nonvolatile residues can be deposited on the TiN sidewalls. These nonvolatile residues are acting like an insulating layer, which can reduce the current density and form a MIM junction. By increasing the  $N_2$  flow rate, the chemical composition of the nonvolatile residues changes and either they become soluble in solvents, they desorb when exposed to the atmosphere, or they become conductive. The absence of an insulating layer on TiN sidewalls after cleaning makes the process suitable for the fabrication of single electron transistors.

## IV. CONCLUSIONS

An ICP etching process for the fabrication of TiN nanostructures over nanotopography is presented. A selectivity of 50 over  $SiO_2$  is achieved with a  $Cl_2/Ar/N_2$  chemistry. Increasing the flow rate of  $N_2$  gas decreases the TiN and ZEP etch rates while also changing the nonvolatile residues deposition on the TiN sidewalls. Current density–voltage measurements proved that for low flow rates of  $N_2$ , an insulating layer is deposited on the TiN sidewalls during the etching. However, for high  $N_2$  flow rates, J-V characteristics confirmed that there was no insulating layer on the trench sidewalls after etching and cleaning, making this process suitable for SET fabrication.

## ACKNOWLEDGMENTS

This work was supported by NSERC, Nanoquebec, and the Regroupement Québécois sur les Matériaux de Pointes (RQMP).

<sup>1</sup>Z. Chen, E. Dubois, F. Ravoux, and F. Danneville, *Microelectron. Eng.* **97**, 280 (2012).

<sup>2</sup>J. Y. Park, J. Y. Kim, Y. D. Kim, H. Jeon, and Y. Kim, *J. Korean Phys. Soc.* **42**, 817 (2003).

<sup>3</sup>W. M. Kim, S. H. Kim, K.-S. Lee, T. S. Lee, and I. H. Kim, *Appl. Surf. Sci.* **261**, 749 (2012).

<sup>4</sup>H. Cui, M. Claes, and S. Suhard, *Solid State Phenom.* **187**, 241 (2012).

<sup>5</sup>C. Dubuc, J. Beauvais, and D. Drouin, *IEEE Trans. Nanotechnol.* **7**, 68 (2008).

<sup>6</sup>S. C. Abraham, C. T. Gabriel, and J. Zheng, *J. Vac. Sci. Technol. A* **15**, 702 (1997).

<sup>7</sup>J. Woo, Y. Joo, J. Park, and C. Kim, *Trans. Electr. Electron. Mater.* **12**, 144 (2011).

- <sup>8</sup>D.-P. Kim, J.-C. Woo, K.-H. Baek, K.-S. Park, K. Lee, K.-S. Kim, and L.-M. Do, *Vacuum* **86**, 380 (2011).
- <sup>9</sup>H. Shin, W. Zhu, L. Liu, S. Sridhar, V. M. Donnelly, D. J. Economou, C. Lenox, and T. Lii, *J. Vac. Sci. Technol. A* **31**, 031305 (2013).
- <sup>10</sup>H. K. Chiu, T. L. Lin, Y. Hu, K. C. Leou, H. C. Lin, M. M. Tsai, and T. Y. Huang, *J. Vac. Sci. Technol. A* **19**, 455 (2001).
- <sup>11</sup>M. Darnon, T. Chevolleau, D. Eon, L. Vallier, J. Torres, and O. Joubert, *J. Vac. Sci. Technol. B* **24**, 2262 (2006).
- <sup>12</sup>M. Darnon *et al.*, *Microelectron. Eng.* **85**, 2226 (2008).
- <sup>13</sup>N. Posseme, R. Bouyssou, T. Chevolleau, T. David, V. Arnal, and M. Darnon, *J. Vac. Sci. Technol. B* **29**, 011018 (2011).
- <sup>14</sup>J. Totonani, T. Iwamoto, F. Sato, K. Hattori, S. Ohmi, and H. Iwai, *J. Vac. Sci. Technol. B* **21**, 2163 (2003).
- <sup>15</sup>A. Le Gouil, O. Joubert, G. Cunge, T. Chevolleau, L. Vallier, B. Chenevier, and I. Matko, *J. Vac. Sci. Technol. B* **25**, 767 (2007).
- <sup>16</sup>S. A. Vitale, J. Kedzierski, and C. L. Keast, *J. Vac. Sci. Technol. B* **27**, 2472 (2009).
- <sup>17</sup>S. C. Heo, D. Yoo, M. S. Choi, D. Kim, C. Chung, and C. Choi, *Jpn. J. Appl. Phys.* **51**, 101203 (2012).
- <sup>18</sup>M. Guilmain, A. Jaouad, S. Ecoffey, and D. Drouin, *Microelectron. Eng.* **88**, 2505 (2011).
- <sup>19</sup>S. R. Min, H. N. Cho, Y. L. Li, S. K. Lm, S. P. Choi, and C. W. Chung, *J. Ind. Eng. Chem.* **14**, 297 (2008).
- <sup>20</sup>A. M. Efremov, D.-P. Kim, and C.-I. Kim, *Thin Solid Films* **435**, 232 (2003).
- <sup>21</sup>R. Gottscho, C. W. Jurgensen, and D. J. Vitkavage, *J. Vac. Sci. Technol. B* **10**, 2133 (1992).
- <sup>22</sup>J.-C. Woo, S.-H. Kim, and C.-I. Kim, *Vacuum* **86**, 403 (2011).
- <sup>23</sup>E. Pargon, O. Joubert, T. Chevolleau, G. Cunge, L. S. Xu, and T. Lill, *J. Vac. Sci. Technol. B* **23**, 103 (2005).
- <sup>24</sup>E. Pargon, O. Joubert, S. Xu, and T. Lill, *J. Vac. Sci. Technol. B* **22**, 1869 (2004).
- <sup>25</sup>M. Guilmain, T. Labbaye, F. Dellenbach, C. Nauenheim, D. Drouin, and S. Ecoffey, *Nanotechnology* **24**, 245305 (2013).